ACS APPLIED MATERIALS & INTERFACES

Research Article

www.acsami.org

Tailoring Hexagonally Packed Metal Hollow-Nanocones and Taper-Nanotubes by Template-Induced Preferential Electrodeposition

Juan Li, Ling Hu, Congshan Li, and Xuefeng Gao*

Suzhou Institute of Nano-Tech and Nano-Bionics, Chinese Academy of Sciences, Suzhou 215123, P. R. China

ABSTRACT: We report a template-induced preferential electrodeposition method for tailoring hexagonally packed metal hollow-nanocones and taper-nanotubes. After sputtering a layer of Au film, anodized aluminum foils with controllable periods and depths of taper-nanopore templates can be directly used as cathodes. Nanonipples on the top-layer of alumina taper-nanopores can cause the "tip effect" during electrodeposition, which makes the metal deposition rate far rapider at the surface of templates than that at the lateral walls and the bottom of nanopores. Accordingly, the pore opening of the template can be rapidly closed while their interior is still hollow. Based on this principle, ordered arrayed of hollow-nanocones with controllable periods (e.g., 100, 200, and 300 nm) and material composition (e.g., Ni, Fe, and Cu) can be realized in a simple, inexpensive, and accessible way. Besides, hexagonally packed metal taper-nanotubes can also be obtained by skillfully making use of the combination of both the "tip effect" and "self-masking" effect of relatively deeper (e.g., 576 nm) taper-nanopores during Au sputtering. Our work opens a door for studying the physical and chemical properties of hexagonally packed hollow-nanocones and tapered-nanotubes made of various metal materials.

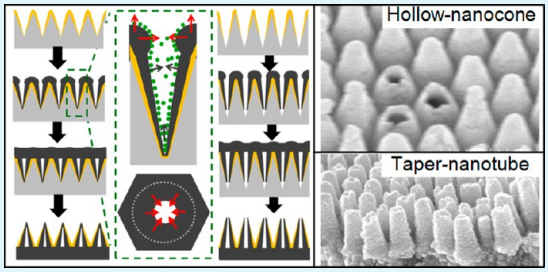

KEYWORDS: *hollow-nanocone, taper-nanotube, electrodeposition, template, porous alumina*

INTRODUCTION

Arrayed nanostructures have attracted intensive interests because of their potential academic and commercial values. In the past two decades, template-assisted methods[1] were demonstrated to be versatile in tailoring different materials of nanostructure arrays.[2−30] In particular, self-ordered porous anodic aluminum oxide (AAO) membranes consisting of naturally formed cylindrical nanopores have been a type of most widely used hard templates because of their advantages in independently controlled structural parameters (i.e., periods, depths, and diameters of nanopores), low-cost large-area processing ability, methodological simplicity, and equipment accessibility.[11,31] To research high-performance magnetics, optics, membrane separation, electrochemical energy storage/conversion devices, sensors, and so on, various deposition methods based on the AAO templates have been developed for tailoring the ordered arrays of metal nanostructures (e.g., nanoscale pores,[11,12] rods,[13−16] tubes,[17−25] wires,[26] and mesochannels[29,30]) with controllable material composition. However, it is still very challenging to tailor the ordered arrays of noncylinder (e.g., tapered) nanostructures with controllable geometrical parameters at a facile and cheap way.[32−35] Recently, Zhao et al.[32] have reported the template-assisted tailoring of Pt conical nanodots by skillfully utilizing the very shallow conical openings of cylindrical alumina nanopores before pore-widening. With technological advance in tailoring the tapered profiles of alumina nanopores,[33−39] solid metal (e.g., Au[33] and Ni[34,35]) nanocones have been obtained. However, their ability in modulating the periods is very limited. Besides, arrays of three-dimensional metal hollow-nanocones and taper-nanotubes are still unreported hitherto, to the best of our knowledge.

Grasping the controllable nanofabrication ability is crucial to develop advanced nanomaterials since the properties of nanomaterials are governed by their architectures (e.g., profiles, periods, and ordering) and chemical compositions. Accordingly, to obtain desired geometrical parameters of hexagonally packed metal hollow-nanocones and taper-nanotubes by classic template-assisted electrodeposition techniques, ones must grasp the ability of tailoring self-ordered taper-nanopore AAO templates. Very recently, our group has made a great breakthrough in continuously tuning the periods of self-ordered alumina taper-nanopores in a broader range (e.g., 70−370 nm), which can be easily realized by one-step hard anodizing and etching peeling of aluminum foils followed by multistep mild anodizing and etching pore-widening.[39] The basic tailoring principle and relationships between the geometrical parameters and reaction conditions under different electrolytes have been well revealed. This method is very facile, cheap, and efficient, dispensing with any aid of external physical process or any costly and/or unavailable equipment, which opens a door for further modulating the periods of metal nanotapers.

It is well-known that, as for electroplating based on conventional cylindrical nanopore alumina templates, scientists and engineers must remove the supporting aluminum substrate and barrier layer to obtain self-standing through-hole membranes

Received: August 21, 2013
Accepted: September 27, 2013
Published: September 27, 2013

with thickness of several ten micrometers, which can be used as the cathodes by further sputtering a layer of Au film. However, this process is not only troublesome and time-consuming but also unsuitable for the taper-nanopore alumina membranes with depths of only several hundred nanometers. These ultrathin self-standing taper-nanopore alumina membranes are very fragile and not so easily to handle. Thus, we wonder if, after simply sputtering a layer of thin Au film, the anodized aluminum foils with taper-nanopore templates can be directly used as the cathodes for tailoring the hexagonally packed metal hollow-nanocones and taper-nanotubes.

Here, we report the controllable fabrication of hexagonally packed metal hollow-nanocones and taper-nanotubes by template-induced preferential electrodeposition methods. After sputtering a layer of Au film, the anodized aluminum foils with controllable periods and depths of taper-nanopore templates can be directly used as the work electrodes. First, nanonipples on the top-layer of alumina taper-nanopores can cause the "tip effect" during electrodeposition,[21] which make the deposition rate of metal ions rapider at the surface of templates than that at the lateral walls and the bottom of nanopores. As a result, the pore opening of the template taper-nanopores can be rapidly closed while their interior is still hollow. Based on this principle, hexagonally packed hollow-nanocones with controllable periods (e.g., 100, 200, and 300 nm) and material composition (e.g., Ni, Fe, and Cu) can be realized in a simple, inexpensive, and accessible way. In addition, the relatively deeper taper-nanopore (e.g., 576 nm) templates can play a "self-masking" effect during Au sputtering, which makes the bottom of pores nearly bare, without the Au deposit. Accordingly, hexagonally packed metal taper-nanotubes can be obtained by skillfully making use of the combination of the "tip effect" and "self-masking" effect. Their formation principles are fully different from the template-assisted methods reported previously, for example, controlling relatively higher revealed current density[17−24] or modifying walls of nanopores with molecular anchors[1] to realize cylindrical nanotubes. Our work opens a door for further studying the novel physical and chemical properties of hexagonally packed hollow-nanocones and tapered-nanotubes made of various metal materials.

RESULTS AND DISCUSSION

The principle of tailoring metal hollow-nanocones and taper-nanotubes based on the taper-nanopore AAO templates is shown in Figure 1. First, the anodized aluminum foils containing taper-nanopores are processed into cathodes by sputtering a layer of Au films. At the initial stage of electrodeposition, metal ions can be simultaneously reduced onto the top-layer surface of templates, the bottom of nanopores, and the lateral walls of nanopores. However, nanonipples at the intersecting places of neighboring nanopores can cause higher local current density due to the well-known "tip effect",[20−22] resulting in far rapider metal deposition rate at the surface of templates than that at the lateral walls of taper-nanopores. Due to two-dimensional honeycomb pattern of top-layer Au films, the preferential metal deposition along the normal and lateral direction of AAO membranes necessarily causes both the "surface-up" thickening and "circle-inward" expansion. Such rapid "circle-inward" expansion of deposited metal layers at the pore opening can dramatically limit the diffusion of ions toward the interior of nanopores, which greatly hinders the "bottom-up" and "wall-up" deposition rates in the interior of nanopores. As a result, the pore opening can be rapidly closed while their interior is still hollow.

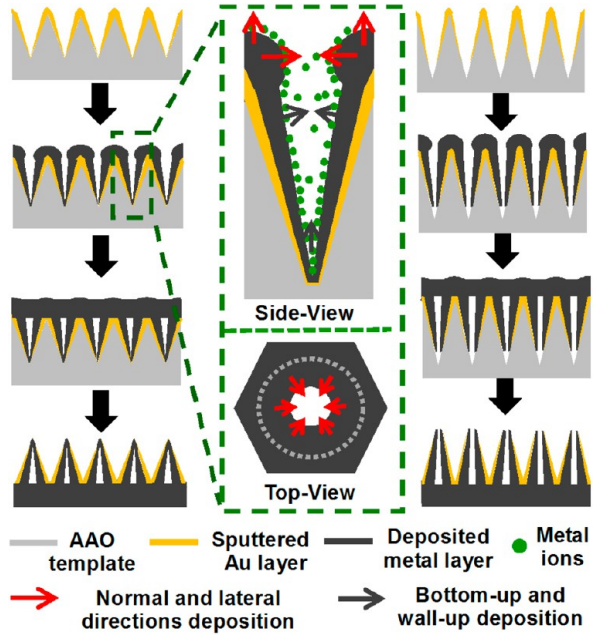

Figure 1. Schematic diagrams of tailoring metal hollow-nanocones and taper-nanotubes by the template-induced preferential electrodeposition. The left shows the principle of tailoring metal hollow-nanocones based on the "tip effect" of top-layer nanonipples during electrodeposition, where the metal deposition rate is far rapider at the surface of templates than these at the lateral walls and the bottom of nanopores. The magnified side-view and top-view of single taper-nanopore at the initial stage of electrodeposition are shown in the middle, respectively. By further skillfully utilizing the "self-masking effect" of deeper taper-nanopores during Au sputtering, the metal hollow-nanocones can be tailored, as shown in the right.

The self-standing metal hollow-nanocones can be obtained after removing the oxide layer and aluminum substrate. Based on the same principle, we can also tailor the ordered arrays of metal taper-nanotubes without top caps by skillfully utilizing the "self-masking effect" of the relatively deeper taper-nanopores during Au sputtering, where a part of pore walls at the bottom are bare without the covering of Au layer.

Exemplified by nickel (Ni), we first obtain the ordered arrays of hollow-nanocones. Figure 2a shows an Au-coated taper-nanopore AAO template with average periods of 200 nm and depths of 389 nm. Through electroplating in a solution of 0.8 M $NiSO_4 \cdot 6H_2O$, 0.3 M $NiCl_2 \cdot 6H_2O$, 0.6 M H_3BO_3, and 0.1 g/L sodium dodecyl sulfate for 3 h, the profiles of AAO taper-nanopores are perfectly replicated by conformal deposition of metal along their surface, as shown in Figure 2b. After removing the AAO templates, we can obtain the self-standing Ni nanocone arrays (Figure 2c). Interestingly, after random mechanical scratch by a steel needle, we can easily demonstrate that the interior of the replicated Ni nanocones is actually hollow, which is clearly seen from the fracture morphologies of some nanocones as shown in Figure 2d and e. X-ray diffraction analyses indicated that the Ni nanocones are crystalline, where the specific diffraction peaks (111), (110), and (112) correspond to the face-centered cubic crystal structure (Figure 2f).[17] It should be pointed out that our studies have demonstrated that the template-induced synthesis of hollow-nanocones is independent of the applied current densities. The as-prepared Ni nanocones are still hollow even as the applied current density is reduced to 10^{-5} A/cm^2.

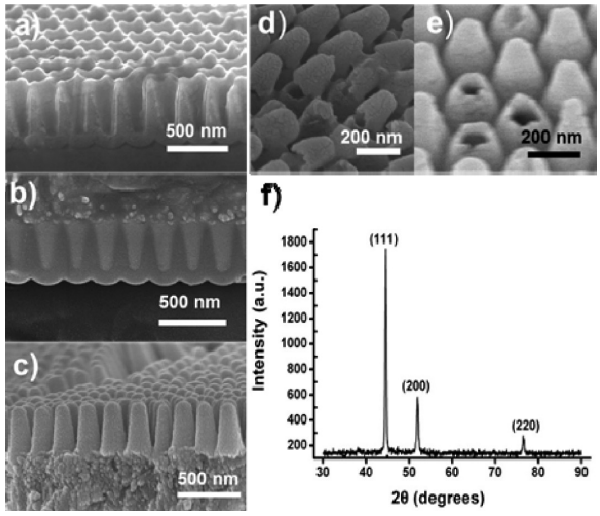

Figure 2. SEM side-views of the Au-coated taper-nanopore AAO template before (a) and after (b) the Ni electrodeposition. (c) SEM side-view of the as-prepared Ni nanocones after removing the template. (d, e) SEM tilted-views of the fractured Ni nanocones, achieved by the random mechanical scratch of a steel needle. (f) XRD pattern of the Ni hollow-nanocones.

To better understand the form mechanism of hollow nanocones, we explored the morphological evolution of the template surface varied with reaction time. As shown in Figure 3,

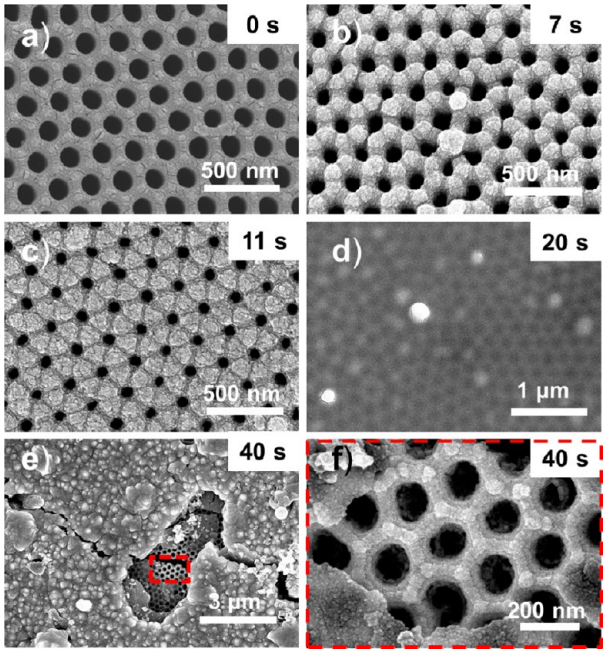

Figure 3. SEM top-views of the surface morphologies of the AAO template after experiencing different electroplating time: (a) 0 s, (b) 7 s, (c) 11 s, (d) 20 s, and (e) 40. (f) Magnified image of the selected area in (e). These data clearly prove that, due to preferential metal deposition at the template surface in contrast to the interior of pores, the pore opening can be rapidly closed at the initial plating stage while their interior is still hollow.

metal deposition along the normal and lateral direction can rapidly cause "surface-up" thickening and "circle-inward" expansion with the extension of plating time. Before plating,

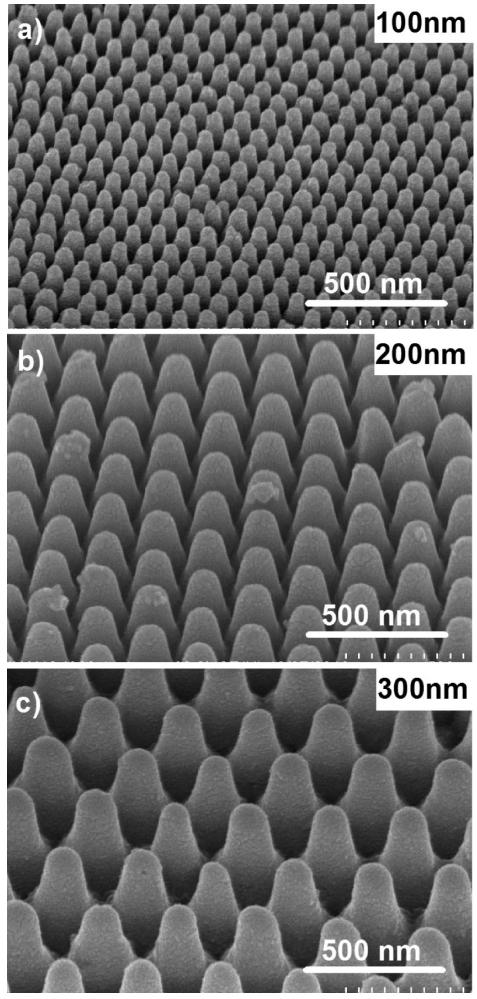

Figure 4. SEM tilted-views of the as-synthesized hexagonally packed Ni hollow-nanocones with controllable periods: (a) 100 nm, (b) 200 nm, and (c) 300 nm. Their periods were governed by the periods of the used taper-nanopore alumina templates.

the initial pore diameter of the AAO template at the pore opening place was 134 ± 3.2 nm (Figure 3a). Remarkably, the pore size can dramatically shrink even after experiencing very short plating. Figure 3b and c shows the pore diameters of 101.9 ± 5.9 and 64.5 ± 6.4 nm, corresponding to the deposition time of only 7 and 11 s, respectively. We found that the template surface had been covered by a translucent thin Ni layer (Figure 3d) as the deposition time reached 20 s. As further extending the plating time to 40 s, the thickness of Ni layer could apparently increase, about several tens of nanometers. As a result, the latent porous structure was no longer clear. The dense metal film could prevent the migration of ions into the taper-nanopores. Very interesting, we occasionally found a broken local (Figure 3e) near the sample edge, which may be ascribed to the fragile nature of Ni layer and the uncontrolled shear force in the process of making sample for scanning electronic microscopic observation. The magnified image of the fractured part can clearly prove that the pore opening can be rapidly closed at the initial plating stage while their interior is still hollow (Figure 3f).

It is easily understood that grasping the ability to control the periods and material composition of hollow-nanocones at a simple, cheap and accessible way are very useful to develop advanced functional nanomaterials and nanodevices with

optimized properties. Herein, we demonstrated that the periods of hollow-nanocones can be easily tuned at this stage, exemplified by the periods of 100, 200, and 300 nm, as shown in Figure 4. For details about tailoring the specific periods of taper-nanopore alumina templates and the corresponding metal hollow-nanocones, see Experimental Section.

Besides, the template-assisted method is suitable for other metal materials due to their inherit merits. Exemplified by Fe and Cu, we can also obtain their hollow nanocones at the hexagonally packed way by electrodeposition in the corresponding electrolyte. Figure 5 shows the scanning electron microscoy (SEM)

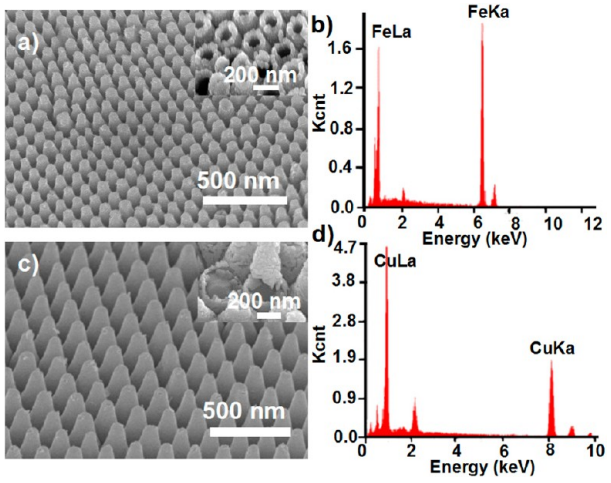

Figure 5. SEM images of the as-synthesized hexagonally packed Fe (a) and Cu (c) hollow-nanocone arrays. The corresponding EDX spectra are shown in (b) and (d). Top-right insets in (a) and (c) clearly show the hollow structure of the as-synthesized metal nanocones.

images and energy dispersive X-ray (EDX) spectra of the as-synthesized hexagonally packed Fe and Cu hollow-nanocone arrays. Their periods are 200 and 375 nm, respectively. The top-right insets in Figure 5a and c clearly show the hollow structure of as-synthesized metal nanocones. It is known that the diameters and depths of alumina nanopores can be easily modulated by controlling chemical etching and anodization time, respectively. Thus, we can provide a facile, cheap, and accessible template-assisted method for tailoring the ordered arrays of hollow-nanocones with controlled structure parameters and material composition.

It is also significant to realize the template-induced tailoring of taper-nanotubes without top caps in many cases. Exemplified by the alumina taper-nanopores with depths of 576 nm, we explored the cross-sectional details of samples after experiencing the Au-sputtering and electroplating treatment, as shown in Figure 6a. The typical "sandwich" structure, consisting of aluminum substrate, Au-coated AAO taper-nanopores and continuous Ni layer, clearly revealed that the bottom of nanopores is still intact, without metal deposition. Self-standing Ni taper-nanotubes were obtained after the template removal. Their SEM top-view and side-view images are shown in Figure 6b and c, respectively. The average heights of the Ni taper-nanotubes are 467 nm, that is, nearly one-fifth of the nanopores of the AAO template had not been filled. Clearly, the failure of Ni electrodeposition at the bottom of nanopores should be attributed to the "self-masking" effect of nanopores during Au sputtering, which makes the pore walls at the bottom bare without the covering of conductive Au layer.

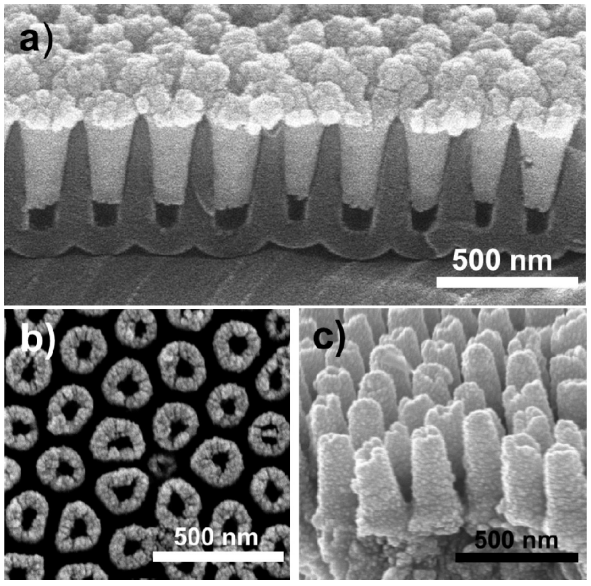

Figure 6. (a) SEM cross-sectional image of taper-nanopore AAO templates with average depths of 576 nm after performing the Ni electrodeposition. The failure of Ni electrodeposition at the bottom of taper-nanopores was ascribed to the "self-masking" effect of nanopores during Au sputtering, which makes the bottom of nanopores bare without covering conductive Au layer. (b, c) SEM top-view and side-view of the as-prepared Ni taper-nanotube arrays after the removal of the AAO templates.

CONCLUSIONS

In summary, we have demonstrated the feasibility of tailoring hexagonally packed metal hollow-nanocones and taper-nanotubes by directly making use of anodized aluminum foils with different depths of taper-nanopores as templates, sputtering a layer of Au film as cathodes and then performing the metal electrodeposition. The formation of metal hollow-nanocones and taper-nanotubes is ascribed to the "tip effect" of nanonipples at the surface of AAO taper-nanopores during electrodeposition and the "self-masking effect" of taper-nanopores during Au sputtering, respectively. Our preliminary studies show that their geometrical parameters and material composition could be easily modulated. Clearly, this general template-induced preferential electrodeposition method is very simple, cheap and accessible to most researchers. Thus, our work opens a door for further studying the physical and chemical properties of hexagonally packed hollow-nanocones and tapered-nanotubes made of various metal materials and developing novel functional nanomaterials and nanodevices with optimal properties, for example, SERS-based sensors[40−42] and energy-conversion devices.[43−46]

EXPERIMENTAL SECTION

Controllable Fabrication of Self-Ordered Taper-Nanopore Alumina Templates. The electropolished highly pure Al foil (99.999%) was first anodized in a mixture solution of mixture of oxalic acid (0.3 M) and sulfuric acid (0.001 M for period of 300 nm, 0.015 M for 200 nm, 0.08 M for 100 nm) at 0−1 °C under a constant voltage of 35 V for 8 min, followed by further anodization by gradually increasing the voltage at 0.5 V s^{-1} until the target value (140 V for 300 nm, 110 V for 200 nm, 80 V for 100 nm). For the templates with periods of 375 nm, a mixture solution of oxalic (0.3) and ethanol (0.34 M) was chosen as the electrolyte, and the target voltage was 170 V. The total anidzation time was 1.5 h. A self-ordered nanopits pattern was left on the sample

surface after removing the porous alumina layer via immersing the samples in a mixed solution of 1.8 wt % CrO_3 and 6 wt % H_3PO_4 at 65 °C for 3 h. The prepatterned samples were then anodized in 0.29 M H_3PO_4 (0.3 M $H_2C_2O_4$) at 10 °C (17 °C) followed by the etching treatment in phosphoric acid solution (0.43 M) at 30 °C for different etching time (20 min for the period 300 nm, 10 min for 200 nm, 8 min for 100 nm, 25 min for 375 nm). The anodization voltages were chosen according to the empirical rules $U_{MA} = D_{int}/2.5$ ($U_{MA} = D_{int}/2$), and each-step anodization time was determined by the depth of the nanopores, from 20 to 300 s. The taper-nanopore AAO templates could be obtained by the five-step anodization and etching treatment. Here, the two-electrode system was used, where the cathode and anode are the Pt disc and aluminum foil, respectively. The sample area is 4.9 cm^2, which corresponds to the alumina templates with diameters of 2.5 cm.

Tailoring Hexagonally Packed Metal Hollow-Nanocones and Taper-Nanotubes by Taper-Nanopore AAO Template-Induced Electrodeposition. The metal electrodeposition was carried out under the constant potential mode in a three-electrode electrochemical cell (CHI 660C, China). The taper-nanopore AAO membrance with aluminum foils were used as the working electrode after sputtering a thin layer of conductive Au films with thickness of ~20 nm, a piece of Pt plate as the counter electrode, and the Ag/AgCl electrode as the reference. All electroplating experiments were performed under the voltage of −1 V for 3 h at 30 °C. The used electroplating baths have three types: Ni-electroplating bath (0.8 M $NiSO_4{\cdot}6H_2O$, 0.3 M $NiCl_2{\cdot}6H_2O$, 0.6 M H_3BO_3, and 0.1 g/L $CH_3(CH_2)_{11}OSO_3Na$), Fe-electroplating bath (250 g/L $FeSO_4$, 150 g/L H_3BO_3, and 25 g/L $C_6H_8O_6$), or Cu-electroplating bath (48 g/L $CuSO_4$ and 12 g/L H_3BO_3). After the electrodeposition, the templates were completely removed by immersing treatment in 1 M NaOH solution. Finally, the samples were obtained by further washing with distilled water and then drying in the oven at 80 °C.

Characterization. The morphologies of the as-prepared metal hollow-nanocones and taper-nanotubes were observed via field-emission scanning electron microscopy (FE-SEM, Hitachi S-4800). Their crystal structure and material composition were measured by X-ray diffraction (XRD, D8 ADVANCE) and energy diffraction X-ray spectra (EDS, Quanta400 FEG), respectively.

AUTHOR INFORMATION

Corresponding Author

*E-mail: xfgao2007@sinano.ac.cn.

Notes

The authors declare no competing financial interest.

ACKNOWLEDGMENTS

This work was supported by National Basic Research Program of China (2012CB933200), National Natural Science Foundation of China (50973081, 91023003, 21104093), and the Key Research Program of Chinese Academy of Sciences (KJZD-EW-M01).

REFERENCES

(1) Martin, C. R. *Science* **1994**, *266*, 1961−1966.
(2) Steinhart, M.; Wehrspohn, R. B.; Gösele, U.; Wendorff, J. H. *Angew. Chem. Int. Ed.* **2004**, *43*, 1334−1344.
(3) Hong, X.; Gao, X.; Jiang, L. *J. Am. Chem. Soc.* **2007**, *129*, 1478−1479.
(4) Choi, K.; Park, S. H.; Song, Y. M.; Lee, Y. T.; Hwangbo, C. K.; Yang, H.; Lee, H. S. *Adv. Mater.* **2010**, *22*, 3713−3718.
(5) Yanagishita, T.; Nishio, K.; Masuda, H. *Appl. Phys. Express* **2008**, *1*, 067004.
(6) Li, J.; Zhou, C.; Jin, X.; Piao, W.; Gao, X. *Chem. Commun.* **2012**, *48*, 11322−11324.
(7) Yanagishita, T.; Endo, T.; Yamaguchi, Y.; Nishio, K.; Masuda, H. *Chem. Lett.* **2009**, *38*, 274−275.
(8) Ergen, O.; Ruebusch, D. J.; Fang, H.; Rathore, A. A.; Kapadia, R.; Fan, Z.; Takei, K.; Jamshidi, A.; Wu, M.; Javey, A. *J. Am. Chem. Soc.* **2010**, *132*, 13972−13974.
(9) Han, F.; Meng, G.; Xu, Q.; Zhu, X.; Zhao, X.; Chen, B.; Li, X.; Yang, D.; Chu, Z.; Kong, M. *Angew. Chem. Int. Ed.* **2011**, *123*, 2084−2088.
(10) Xiao, F. *Chem. Commun.* **2012**, *48*, 6538−6540.
(11) Masuda, H.; Fukuda, K. *Science* **1995**, *268*, 1466−1468.
(12) Yanagishita, T.; Nishio, K.; Masuda, H. *Adv. Mater.* **2005**, *17*, 2241−2243.
(13) Masuda, H.; Abe, A.; Nakao, M.; Yokoo, A.; Tamamura, T.; Nishio, K. *Adv. Mater.* **2003**, *15*, 161−164.
(14) Li, F.; Zhou, M.; Liu, C.; Zhou, W. L.; Wiley, J. B. *J. Am. Chem. Soc.* **2006**, *128*, 13342−13343.
(15) Yoo, S. -H.; Park, S. *Adv. Mater.* **2007**, *19*, 1612−1615.
(16) Huang, Z.; Meng, G.; Huang, Q.; Yang, Y.; Zhu, C.; Tang, C. *Adv. Mater.* **2010**, *22*, 4136−4319.
(17) Bao, J.; Tie, C.; Xu, Z.; Zhou, Q.; Shen, D.; Ma, Q. *Adv. Mater.* **2001**, *13*, 1631−1633.
(18) Mu, C.; Yu, Y.; Wang, R.; Wu, K.; Xu, D.; Guo, G. *Adv. Mater.* **2004**, *16*, 1550−1553.
(19) Sander, M. S.; Gao, H. *J. Am. Chem. Soc.* **2005**, *127*, 12158−125159.
(20) Yoo, W. -C.; Lee, J.-K. *Adv. Mater.* **2004**, *16*, 1097−1101.
(21) Lee, W.; Scholz, R.; Nielsch, K.; Gösele, U. *Angew. Chem. Int. Ed.* **2005**, *44*, 6050−6054.
(22) Cao, H.; Wang, L.; Qiu, Y.; Wu, Q.; Wang, G.; Zhang, L.; Liu, X. *ChemPhysChem* **2006**, *7*, 1500−1504.
(23) Cui, G.; Zhi, L.; Thomas, A.; Kolb, U.; Lieberwirth, I.; Müllen, K. *Angew. Chem. Int. Ed.* **2007**, *46*, 3464−3467.
(24) Han, X. -F.; Shamaila, S.; Sharif, R.; Chen, J. -Y.; Liu, H. -R.; Liu, D. -P. *Adv. Mater.* **2009**, *21*, 4619−4624.
(25) Liu, H.; Li, Y.; Jiang, L.; Luo, H.; Xiao, S.; Fang, H.; Li, H.; Zhu, D.; Yu, D.; Xu, J.; Xiang, B. *J. Am. Chem. Soc.* **2002**, *124*, 13370−13371.
(26) Guo, Y.; Tang, Q.; Liu, H.; Zhang, Y.; Li, Y.; Hu, W.; Wang, S.; Zhu, D. *J. Am. Chem. Soc.* **2008**, *130*, 9198−9199.
(27) Cui, S.; Liu, H.; Gan, L.; Li, Y.; Zhu, D. *Adv. Mater.* **2008**, *20*, 2918−2925.
(28) Liu, H.; Xu, J.; Li, Y.; Li, Y. *Acc. Chem. Res.* **2010**, *43*, 1496−1508.
(29) Yamauchi, Y.; Nagaura, T.; Inoue, S. *Chem.—Asian J.* **2009**, *4*, 1059−1063.
(30) Yamauchi, Y. *J. Ceram. Soc. Japan* **2013**, *121*, 831−840.
(31) Li, A. P.; Müller, F.; Birner, A.; Nielsch, K.; Gösele, U. *J. Appl. Phys.* **1998**, *84*, 6023−6026.
(32) Zhao, S.; Roberge, H.; Yelon, A.; Veres, T. *J. Am. Chem. Soc.* **2006**, *128*, 12352−12353.
(33) Yamauchi, Y.; Wang, L.; Ataee-Esfahani, H.; Fukata, N.; Nagaura, T.; Inoue, S. *J. Nanosci. Nanotechnol.* **2010**, *10*, 4384−4387.
(34) Nagaura, T.; Takeuchi, F.; Yamauchi, Y.; Wada, K.; Inoue, S. *Electrochem. Commun.* **2008**, *10*, 681−685.
(35) Yamauchi, Y.; Nagaura, T.; Takai, K.; Suzuki, N.; Sato, K.; Fukata, N.; Inoue, S.; Kishimoto, S. *J. Phys. Chem. C* **2009**, *113*, 9632−9637.
(36) Yanagishita, T.; Yasui, K.; Kondo, T.; Kawamoto, Y.; Nishio, K.; Masuda, H. *Chem. Lett.* **2007**, *36*, 530−531.
(37) Yamauchi, Y.; Nagaura, T.; Ishikawa, A.; Chikyow, T.; Inoue, S. *J. Am. Chem. Soc.* **2008**, *130*, 10165−10169.
(38) Li, C.; Li, J.; Chen, C.; Gao, X. *Chem. Commun.* **2012**, *48*, 5100−5102.
(39) Li, J.; Li, C.; Chen, C.; Hao, Q.; Wang, Z.; Zhu, J.; Gao, X. *ACS Appl. Mater. Interfaces* **2012**, *4*, 5678−5683.
(40) Sun, C.-H.; Linn, N. C.; Jiang, P. *Chem. Mater.* **2007**, *19*, 4551−4556.
(41) Gao, H.; Zhou, W.; Odom, T. W. *Adv. Funct. Mater.* **2010**, *20*, 529−539.
(42) Yang, J. -C.; Gao, H.; Suh, J. Y.; Zhou, W.; Lee, M. H.; Odom, T. W. *Nano Lett.* **2010**, *10*, 3173−3178.
(43) Nishizawa, M.; Menon, V. P.; Martin, C. R. *Science* **1995**, *268*, 700−702.
(44) Siwy, Z. S. *Adv. Funct. Mater.* **2006**, *16*, 735−746.
(45) Xu, J.; Lavan, D. A. *Nat. Nanotechnol.* **2008**, *3*, 666−670.
(46) Hou, X.; Guo, W.; Jiang, L. *Chem. Soc. Rev.* **2011**, *40*, 2385−2401.